

Mapping whitebark pine mortality caused by a mountain pine beetle outbreak with high spatial resolution satellite imagery

JEFFREY A. HICKE*† and JESSE LOGAN‡

†Department of Geography, University of Idaho, Moscow, ID 83843, USA

‡USDA Forest Service (retired), Rocky Mountain Research Station, Logan, UT 84321, USA (now at: EnviroWise Design, Emigrant, MT 59027, USA)

(Received 27 May 2008; in final form 8 October 2008)

Insect outbreaks cause significant tree mortality across western North America, including in high-elevation whitebark pine forests. These forests are under several threats, which include attack by insects and white pine blister rust, as well as conversion to other tree species as a result of fire suppression. Mapping tree mortality is critical to determining the status of whitebark pine as a species. Satellite remote sensing builds upon existing aerial surveys by using objective, repeatable methods that can result in high spatial resolution monitoring. Past studies concentrated on level terrain and only forest vegetation type. The objective of this study was to develop a means of classifying whitebark pine mortality caused by a mountain pine beetle infestation in rugged, remote terrain using high spatial resolution satellite imagery. We overcame three challenges of mapping mortality in this mountainous region: (1) separating non-vegetated cover types, green and brown herbaceous cover, green (live) tree cover, and red-attack (dead) tree cover; (2) variations in illumination as a result of variations in slope and aspect related to the mountainous terrain of the study site; and (3) the difficulty of georegistering the imagery for use in comparing field measurements. Quickbird multi-spectral imagery (2.4 m spatial resolution) was used, together with a maximum likelihood classification method, to classify vegetation cover types over a 6400 ha area. To train the classifier, we selected pixels in each cover class from the imagery guided by our knowledge of the study site. Variables used in the maximum likelihood classifier included the ratio of red reflectance to green reflectance as well as green reflectance. These variables were stratified by solar incidence angle to account for illumination variability. We evaluated the results of the classified image using a reserved set of image-derived class members and field measurements of live and dead trees. Classification results yielded high overall accuracy (86% and 91% using image-derived class members and field measurements respectively) and kappa statistics (0.82 and 0.82) and low commission (0.9% and 1.5%) and omission (6.5% and 15.9%) errors for the red-attack tree class. Across the scene, 700 ha or 31% of the forest was identified as in the red-attack stage. Severity (percent mortality by canopy cover) varied from nearly 100% for some areas to regions with little mortality. These results suggest that high spatial resolution satellite imagery can provide valuable information for mapping and monitoring tree mortality even in rugged, mountainous terrain.

*Corresponding author. Email: jhicke@uidaho.edu

1. Introduction

Outbreaks of mountain pine beetle (*Dendroctonus ponderosae* Hopkins) affect large areas in western North America. In recent years, these insects have killed trees in >1 million ha in the western USA (USDA Forest Service 2005) and 9 million ha in western Canada (British Columbia Ministry of Forests and Range 2007). Future outbreaks will likely be extensive and severe in western North America. Over 8 million ha of western forests are at a high risk of mortality caused by bark beetles, including mountain pine beetle (USDA Forest Service 2002), and 46% of the lodgepole pine in the USA has stand conditions that are highly susceptible to mountain pine beetle attack (Hicke and Jenkins 2008). Projections of future warming will enhance climate suitability for mountain pine beetle epidemics in high-elevation pine ecosystems (Logan and Bentz 1999, Logan *et al.* 2003, Hicke *et al.* 2006). Tree mortality associated with insect disturbance has numerous ecosystem impacts, including carbon cycling (Romme *et al.* 1986, Kurz and Apps 1999, Kurz *et al.* 2008), streamflow (Bethlahmy 1974), fire (Romme *et al.* 2006, Jenkins *et al.* 2008) and wildlife habitat (Chan-McLeod 2006).

Mountain pine beetles typically attack lodgepole pine (*Pinus contorta*), ponderosa pine (*Pinus ponderosa*), and other pines, such as whitebark pine (*Pinus albicaulis*) (Amman and Cole 1983). Needles on successfully attacked and killed trees begin to fade the following spring and summer, turning bright red then falling off in 3–5 years. Trees progress through unattacked, green-attack (attacked but needles still green), red-attack (dead, needles red), and grey-attack (dead, needles off) stages (Safranyik and Carroll 2006). In this study, we focus on identifying forest cover in the red-attack stage.

Whitebark pine is a foundation species of high-elevation ecosystems in the western USA. Whitebark pine serves a variety of ecological roles, including providing food resources for grizzly bears, squirrels and birds and modifying hydrological processes through effects on snowpack. Whitebark pine is currently subjected to numerous threats, which include epidemics of mountain pine beetle, white pine blister rust and, in some places, conversion to later seral species resulting from fire suppression (Keane and Arno 1993, Logan and Powell 2001).

Until recently, whitebark pine ecosystems were usually too cold to support frequent mountain pine beetle epidemics. However, during warmer periods, such as the 1930–1940s, mountain pine beetle populations reached epidemic levels (Perkins and Swetnam 1996, Logan and Powell 2001). In 2005 alone, mountain pine beetles attacked over 170 000 ha of whitebark pine surveyed by the USDA Forest Service in the Greater Yellowstone Ecosystem (Gibson 2006). Other areas of whitebark pine are also infested, including locations throughout Idaho. Ongoing warming today is thought to be responsible (Logan and Powell 2001, *in press*), and projections of mountain pine beetle activity at high elevations that are driven by climate change forecasts suggest continued optimal conditions for outbreak for many decades (Hicke *et al.* 2006).

Two sources of information can be useful for mapping insect outbreaks across a landscape. The USDA Forest Service annually surveys forests for insect and disease damage, producing maps and attribute information. From fixed-wing aircraft, observers visually identify areas of insect and disease damage, together with an estimate of the number of trees affected. Although a rich resource, these Aerial Detection Surveys have disadvantages for ecological studies. Many areas are flown annually, though some areas can be missed, and wildernesses and national parks are not surveyed regularly. Traditionally, surveys have focused on valued timber species; only recently

have the surveys included additional tree species, such as whitebark pine. The method involves an observer mapping damage and, as such, is subjective and not repeatable, although with experienced observers the accuracy of detection and location of outbreaks can be high (Van Sickle 1995). Though suitable for the Forest Service purposes of early warning and general trends, the spatial resolution of the mortality locations is too coarse for many ecological studies.

The usefulness of remote sensing imagery in studying forest mortality resulting from outbreaks is widely recognized (Radeloff *et al.* 1999, Franklin *et al.* 2003, Skakun *et al.* 2003, Wulder *et al.* 2006). However, insect-caused mortality is more difficult to detect from space than other forest disturbances, such as fire or clear-cutting. Outbreaks leave living younger trees, non-host species and the understorey, resulting in a mixture of reflectances from live and dead trees. A major factor influencing the ability of remotely sensed data to detect infestation is the spatial resolution of the imagery. Past studies of detection using remote sensing have indicated that finer spatial resolution results in fewer pixels with mixed live and killed trees, facilitating detection (e.g. Knepeck and Ahern 1989, Wulder *et al.* 2006). Recent studies using high spatial resolution (2–4 m) satellite imagery have demonstrated success in mapping red-attack damage resulting from mountain pine beetle outbreaks (White *et al.* 2005, Coops *et al.* 2006, Wulder *et al.* 2008). These studies have been conducted in relatively level terrain in British Columbia in areas of extensive forest cover.

Satellite remote sensing is a particularly valuable monitoring tool in whitebark pine stands for three reasons. First, whitebark pines are often located in national parks and wildernesses, areas not regularly flown by aerial surveys but available to satellites. Secondly, the remote, rugged terrain characterizing whitebark pine stands is difficult to survey with ground-based methods. Thirdly, mortality mapped with satellite imagery can be characterized continuously across a landscape at potentially high spatial resolution.

Our overall goal is to develop the means of mapping mountain pine beetle-caused tree mortality in rugged, remote areas for monitoring the status of whitebark pine. In this paper, we describe a classification of satellite imagery to identify whitebark pine mortality resulting from mountain pine beetle attack at Railroad Ridge in central Idaho, USA. The mountain pine beetle infestation began in the area around 2003 and is ongoing. Our specific objectives were to (1) develop a classification method for mapping mortality in whitebark pine stands, (2) evaluate the classification using image-derived information and field measurements and (3) report the total area of mortality both in absolute area as well as a percentage of total forest. We focused on live (green) and dead (red-attack) tree cover. Our study builds upon previously published reports of mapping tree mortality following insect attack by developing and applying methods for use in mountainous terrain. We addressed three challenges for such areas: (1) separating non-vegetated surfaces, green and brown herbaceous cover, green (live) tree cover, and red-attack (dead) tree cover using the imagery (due to the lack of ancillary information); (2) variations in illumination that result from highly variable slope and aspect; and (3) the difficulty of georegistering the imagery in this rugged terrain, which led to uncertainty in comparing classification results with field observations.

2. Study region

The study site is centred on Railroad Ridge, Idaho, USA (44.140°N, 114.556°W) in the White Cloud Peaks area east of Stanley, Idaho (figure 1). The region is characterized by remote, rugged terrain. Elevations range from 2042 m to above treeline at 3505 m,

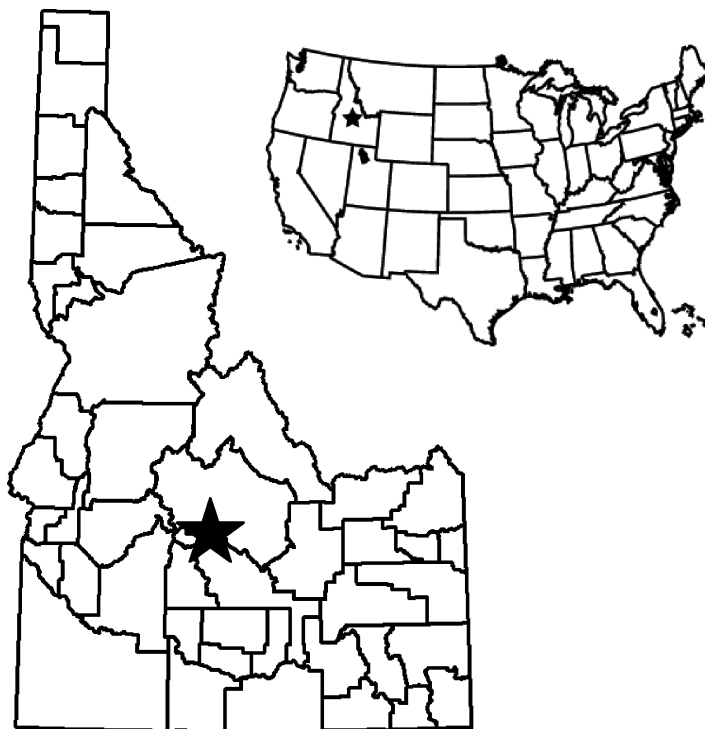


Figure 1. Study site: Railroad Ridge in central Idaho, USA (44.140°N , 114.556°W) (star).

with slopes averaging 23° and a ranging from 0° to $>60^{\circ}$ (figure 2). Land-cover types across the study site include lakes, talus/rock, herbaceous vegetation in alpine and subalpine meadows, and coniferous forest. Lodgepole pine occurs at lower elevations, whitebark pine dominates forests at higher elevations up to treeline, and subalpine fir is present in low densities.

The ongoing mountain pine beetle outbreak at Railroad Ridge began in 2003, with increasing mortality in each subsequent year, according to visual estimates. Mountain pine beetles have killed both whitebark pine as well as lodgepole pine within the study site.

3. Methods

3.1 Image preprocessing

A Quickbird multi-spectral image was acquired on 13 July 2005, at Railroad Ridge over an 8 km by 8 km region. The imagery has a spatial resolution of 2.4 m for the multi-spectral bands (blue, green, red, near-infrared) and a view zenith angle of 2.4° . The scene was mostly clear, with a small amount of cloud in the south-east corner.

Orthorectification and georegistration were performed with the Environment for Visualization Images (ENVI) software package using rational polynomial coefficients provided with the Quickbird imagery together with field-measured ground control points and a digital elevation model (DEM). Two issues made orthorectification and geolocation challenging in this scene. First, regular, human-produced features, such as paved roads, fences and buildings that facilitate identification on imagery, were not

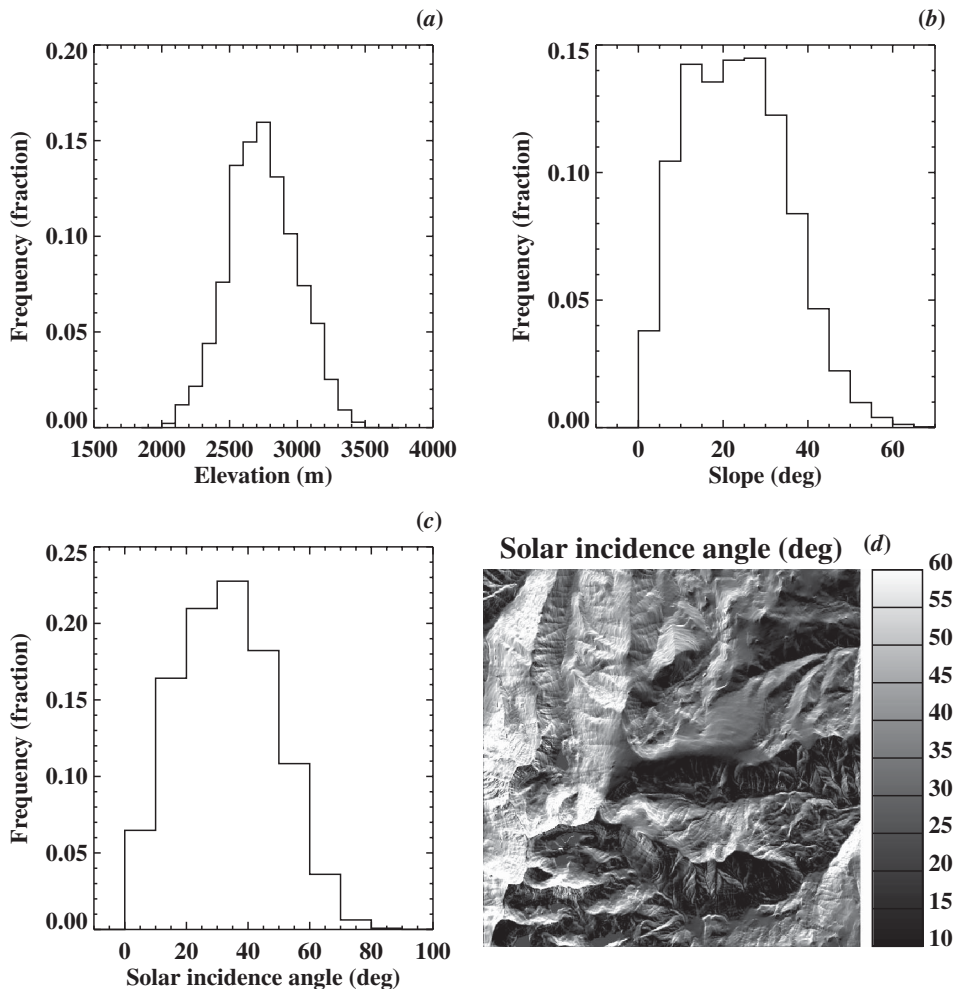


Figure 2. (a) Elevation frequency distribution at Railroad Ridge; (b) slope frequency distribution; (c) solar incidence angle (SIA; defined as the angular difference between the Sun and a perpendicular to the local surface) frequency distribution; and (d) map of SIA across study site. The study region consists of rugged, mountainous terrain, which influences solar illumination and orthorectification.

present in this landscape. Secondly, this region is characterized by complex terrain with steep mountains and substantial gradients in elevation. Twenty-three ground control points distributed across the scene were taken at (one-lane, unpaved) road intersections, stream crossings and solitary trees and logs with a Trimble Pathfinder Pro XRS Global Positioning System (GPS) receiver. Differential correction was applied to these points. We downloaded 10 m United States Geological Survey (USGS) DEMs for the region, then linearly interpolated the 10 m grid cells to match the 2.4 m spatial resolution of the satellite imagery for use in the orthorectification. An assessment of pre- and post-orthorectification positions of these points revealed a rms. error of 2.1 pixels or 5.0 m. Comparisons of field GPS points with USGS digital orthophotographs revealed similar errors in the orthophotographs.

Top-of-atmosphere digital numbers were converted to top-of-atmosphere spectral reflectances using the spectral response and calibration coefficients of each band and the solar spectrum. Top-of-canopy reflectances were estimated from these reflectances using the 6S radiative transfer model (Vermote *et al.* 1997) assuming a standard US atmospheric profile. Although not needed for the classification, this step facilitated interpretation of the reflectance spectra.

From the mosaicked DEM and the position of the Sun at the time of image acquisition, we calculated the ‘solar incidence angle’ (SIA) that characterized the angular difference between a local perpendicular at each pixel and the incoming solar radiation:

$$\cos \text{SIA} = \cos \alpha \cos \beta - \sin \alpha \sin \beta \sin \phi \quad (1)$$

where α is the solar zenith angle, β is the slope and ϕ is the solar azimuth angle. SIA was used in the classification to capture the variations in reflectance resulting from variability in slope and aspect. We designated five SIA bins across the study region: 0–15°, 15–30°, 30–45°, 45–60° and 60–75°.

3.2 Image classification

We first removed cover types other than vegetation (rock, water, cloud) from consideration by applying a minimum normalized difference vegetation index (NDVI) threshold (figure 3 shows a flow diagram of the classification process). Based on visual inspection of the imagery and our knowledge of the study site, we retained for use in subsequent analysis only those pixels whose $\text{NDVI} \geq 0.22$. Since

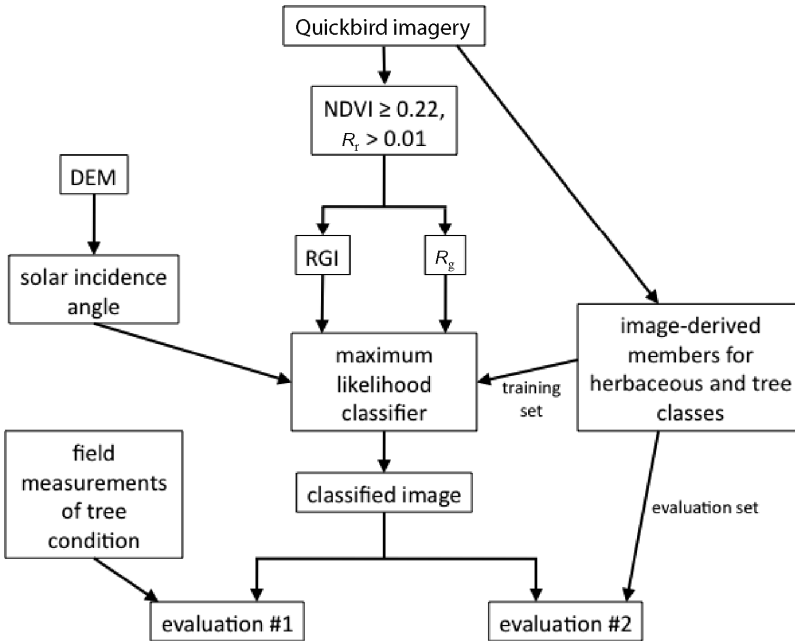


Figure 3. Flow diagram of classification of Quickbird imagery to yield locations of green and brown herbaceous vegetation and green and red-attack tree cover. RGI, red–green index; DEM, digital elevation model.

areas of cloud and water had NDVI values greater than this threshold, we also applied a minimum threshold of 0.01 for the reflectance of red band to remove these additional areas.

Next, we used a maximum likelihood classification method to identify four vegetation classes: green and brown herbaceous cover, and green (live) and red-attack (dead) tree cover. We began by selecting pixels from the imagery to build training and evaluation datasets for use in the classification. Using our local knowledge of the vegetation at the study site and the satellite imagery displayed in true colour, we visually selected pixels ('class members') of each vegetation class from the imagery. We ensured representation of these pixels across the five SIA bins described above. We then randomly selected two-thirds of the points for model training and reserved the remaining third for model evaluation. Random selection considered SIA (five bins) as well as the two variables used in the maximum likelihood classification (the red-green index, RGI, and the green reflectance, R_g (see below); four equal-sized bins of each). This stratification among $5 \times 4 \times 4 = 80$ bins ensured representation across the range of these three variables for model training and evaluation.

RGI alone has been used successfully to separate the red-attack from live tree locations, and was found to be superior to NDVI for this discrimination (Coops *et al.* 2006). However, our study region included herbaceous vegetation in addition to trees, and no ancillary data existed that would have allowed us to mask out non-forest areas. RGI does not discriminate between herbaceous and tree cover classes (figure 4). Therefore, we added the green reflectance (R_g) as a classification variable, which allowed us to separate herbaceous vegetation from tree cover (figure 4).

These two variables (RGI, R_g) were used in the maximum likelihood classification of the Quickbird imagery (Richards and Jia 2006). Class means were computed using the training set of image-derived class members. However, we found

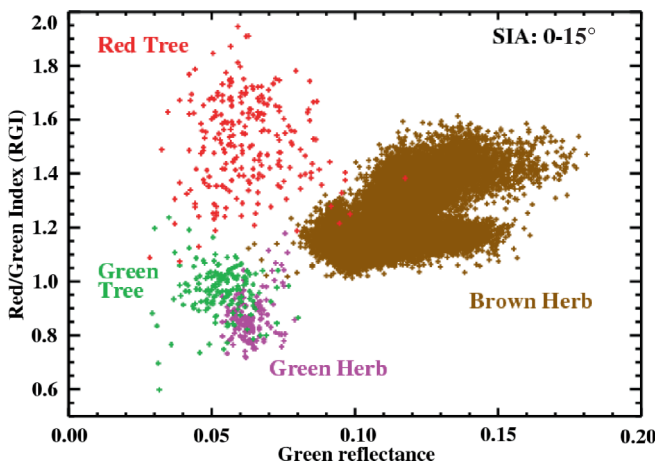


Figure 4. Green reflectance versus the ratio of red to green reflectance (RGI, red-green index) for the four image-derived class members. Class members are limited to those with solar incidence angles (SIA) between 0° and 15° . Note that RGI alone is insufficient for distinguishing brown herbaceous cover from red and green tree cover, but that the addition of green reflectance permits this separation.

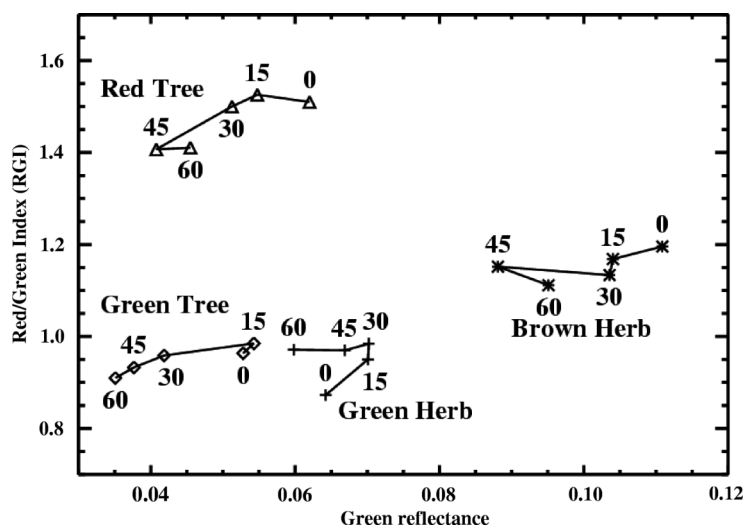


Figure 5. Green reflectance versus the ratio of red to green reflectance (RGI, red-green index) for means of the four image-derived classes stratified by solar incidence angle (SIA). Numbers indicate lower SIA of each SIA bin: 0: 0–15°; 15: 15–30°; 30: 30–45°; 45: 45–60°; 60: 60–75°. Class means of RGI and green reflectances vary with SIA, implying that SIA needed to be accounted for in the classification process.

that these class means varied with SIA (figure 5). R_g decreased as SIA increased in response to reduced illumination and increased shadowing. RGI also decreased, though it was less sensitive than R_g . To account for this variability in the training datasets caused by changing SIA, we performed one maximum likelihood classification for each of the five SIA bins. That is, we selected training class members and imagery pixels within a given SIA bin to perform each classification; we then repeated this step for each SIA bin.

After performing the classification, we noted a significant number of small patches of red-attack pixels. Coops *et al.* (2006) reported a mean crown radius of 1.7 m for lodgepole pine in British Columbia and, therefore, used four Quickbird pixels to represent a crown. Whitebark pine crowns are typically larger; one study reported crown diameters between 4.7 and 12.1 m, with a mean of 8.5 m (Caylor *et al.* 2002). We therefore removed patches containing fewer than four pixels from consideration. Instead of the red-attack class, we assigned the second-most likely class to these pixels.

3.3 Classification evaluation

We used two methods of evaluating the classification because each method has advantages and disadvantages, and a combination of the two increases the confidence of our results. Image-derived class members provided a large number of locations for evaluation, but relied upon visual selection from the Quickbird imagery. Field measurements quantified tree condition from ground-based observations but rectification with the imagery was difficult.

The reserved set (third of total) of image-derived class members was used to evaluate the classification. Since the numbers of pixels in each class varied substantially, we limited each class to 462 pixels, the number in the red-attack class, by

random selection. An error matrix was calculated using pixels from the classification results compared with the image-derived class members. We report overall accuracy, the kappa statistic, user's and producer's accuracy, and percent commission and omission errors.

In addition, field measurements were used for evaluation. Coordinates of 207 green (live) and 232 red (dead) trees were taken throughout the study site with the Trimble GPS receiver in September 2005. Tree coordinates were measured in plots established for studying mountain pine beetle populations as well as in a variety of slope-aspect combinations. We followed a protocol that measured coordinates 1 m from the south side of each tree bole. Differential correction was applied after the field trip; reported horizontal precision was typically <1 m. Information about each tree, including species, condition (live or dead) and colour (green, red, grey; only green and red trees were used in this study), was recorded.

We developed an accuracy assessment approach to compare GPS points of live and dead trees with the satellite classification. We needed to consider a number of issues that led to uncertainties in the comparisons. These issues included (listed in order of importance): (1) orthorectification rms. error of two pixels; (2) variations in crown orientation with respect to the base of the stem, which can be particularly large in whitebark pine when, as we regularly observed, multiple mature stems originated within a small area on the ground from bird caches; (3) precision of the GPS points (typically <1 m); and (4) variations in crown width. These issues implied that directly comparing a GPS point with the overlying satellite pixel might not be a meaningful test. Therefore, with the orthorectification uncertainty of two pixels as a guide, we used an image window of 5×5 pixels to look for a match between the ground-recorded tree condition (live or dead) and satellite classification within each window. White *et al.* (2005) used a similar method for accuracy assessment by adding a buffer around ground observations to account for positional errors in 4 m IKONOS imagery. A similar analysis of the resulting error matrix as for the image-derived evaluation dataset was performed.

4. Results

From our classification of Railroad Ridge Quickbird imagery, we estimated 2264 ha of total forest (green/live plus red/dead) across the 6400 ha scene (35%). The remainder of the scene consisted of large areas of non-vegetation cover types, mostly rock, and brown herbaceous cover, with a small amount of green herbaceous cover (figure 6).

We found 700 ha of forest in the red-attack stage killed by mountain pine beetle, or 31% of the total forest area. Much of the mortality was in the north-central and north-eastern parts of the scene. Less mortality occurred in the north-western region. However, we identified some red-attack areas in stands throughout most of the scene.

The evaluation against image-derived class members yielded an overall accuracy of 86% and a kappa statistic value of 0.82 (table 1). Focusing on the red-attack class – the object of this study – we found low commission errors (0.9%) and omission errors (6.5%). The brown herbaceous cover type had similarly low commission and omission errors. The green herbaceous and green tree cover types had larger errors, implying that the classification method did not distinguish these two classes well.

Comparisons of the classified imagery with field observations of green and red trees resulted in an overall accuracy of 91% and a kappa statistic value of 0.82. The

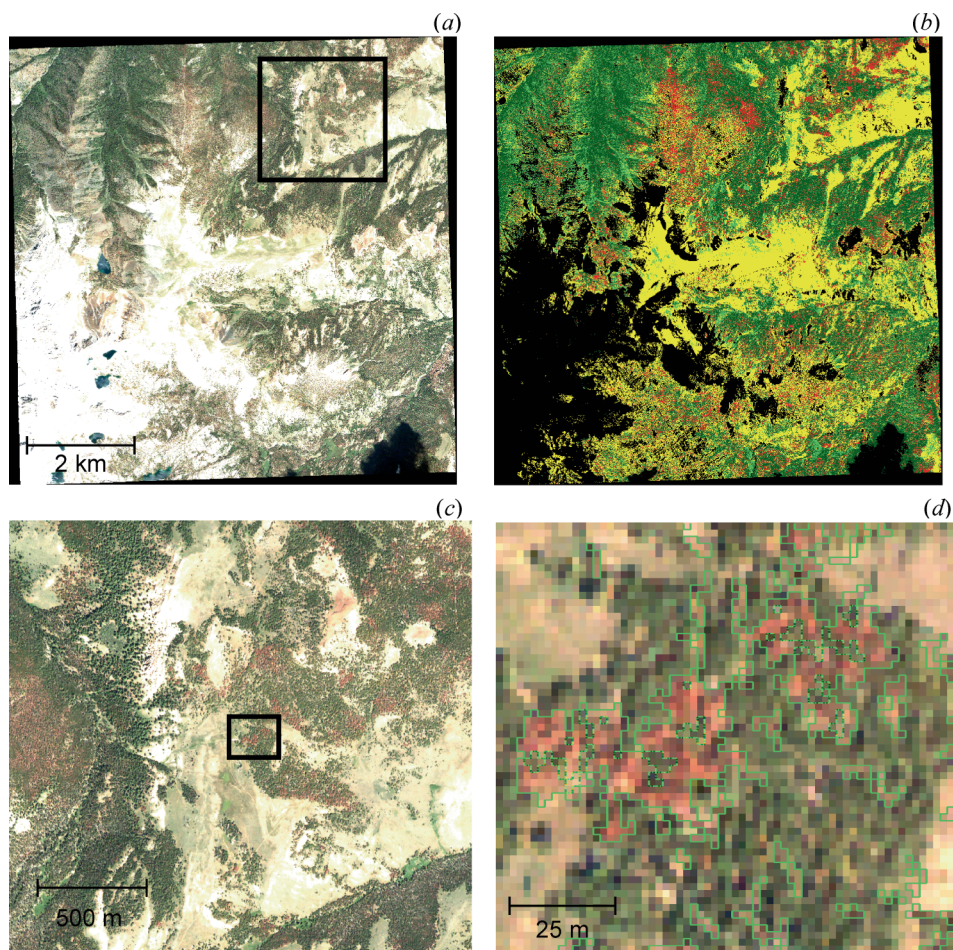


Figure 6. (a) True-colour Quickbird imagery of entire Railroad Ridge study site (8 km by 8 km). (b) Classification results of entire study site: light green: green herbaceous cover; yellow: brown herbaceous cover; dark green: green (live) tree cover; red: red-attack tree cover. (c) Zoom of true-colour imagery; region in black box in (a) shown. (d) Zoom of true-colour imagery; region in black box in (c) shown. Green lines outline red-attack tree class (dashed lines indicate holes). Imagery courtesy of DigitalGlobe Inc., Longmont CO, © 2005.

commission error of red-attack trees was low (1.5%), and the omission error was low, but slightly higher (15.9%). Errors primarily occurred because the classification mistakenly assigned red-attack trees (as observed in the field) to the green tree cover class.

5. Discussion

Our method satisfactorily separated the red-attack class from herbaceous and live tree classes by using RGI, R_g , and SIA based on evaluations using image-derived class members (table 1) and field observations (table 2). We found low omission and commission errors for this cover type from both image-derived class members and

Table 1. Error matrix using image-derived class members.

	Reference (image-derived class members)				Total	User's accuracy (%)	Commission error (%)
	Green herb.	Brown herb.	Green tree cover	Red tree cover			
Classified							
Green herb.	343	9	90	6	448	76.6	23.4
Brown herb.	61	429	3	5	498	86.1	13.9
Green tree cover	58	0	363	16	437	83.1	16.9
Red tree cover	0	0	4	432	436	99.1	0.9
Total	462	462	462	462	1819		
Producer's accuracy (%)	74.2	92.9	78.6	93.5		Overall accuracy	86.14%
Omission error (%)	25.8	7.1	21.4	6.5		kappa	0.82

Table 2. Error matrix using field measurements.

	Reference (field measurements)				User's accuracy (%)	Commission error (%)
	Green tree	Red tree	Other	Total		
Classified						
Green tree cover	204	35	0	239	85.4	14.6
Red tree cover	3	195	0	198	98.5	1.5
Other ^a	0	2	0	2	0.0	100.0
Total	207	232	0	439		
Producer's accuracy (%)	98.6	84.1	-		Overall accuracy	90.9%
Omission error (%)	1.4	15.9	-		kappa	0.82

^aThe 'other' class includes non-vegetation and herbaceous cover types.

field observations. Other cover types were less well distinguished. Green herbaceous cover and green tree cover classes were most problematic due to their similar RGI and R_g characteristics (figure 4). We did not distinguish between a live, unattacked tree cover class and a green-attack tree cover class. In addition, we did not consider the grey-attack stage; this topic will be addressed in future studies. The lack of including green- and grey-attack classes suggests additional mortality across the scene that was not captured by our methods.

A high degree of accuracy compared with the field observations of live and dead trees was achieved once uncertainties in spatial positioning of the imagery and the GPS points (relative to a tree's crown) were included. Most significantly, the lack of regularly shaped (e.g. rectangular), easily identified human features in this landscape, lack of easy access, and steep topography reduced our ability to accurately and precisely georegister the Quickbird imagery. We recognize that this method of using a 5×5 window may overestimate the accuracy because of the possibility of including a match not associated with the tree of interest.

In addition to location uncertainties, in the field we observed additional fading between the time of Quickbird imagery acquisition (July) and fieldwork (September). Visual assessment in the field identified some trees obviously green in the July true-colour imagery that were red in September. This additional fading likely increased the red-attack class omission error (table 2).

High accuracies have also been reported by studies using high-resolution satellite imagery to map tree mortality following bark beetle attack. Coops *et al.* (2006) used multi-spectral Quickbird imagery to classify red-attack trees. Individual spectral bands as well as RGI and NDVI were evaluated. An iterative process determined RGI and NDVI thresholds in conjunction with a dataset of attacked trees identified from helicopter GPS points. The authors found that RGI was most successful in separating the red-attack stage from unattacked (green) locations. White *et al.* (2005) focused on the usefulness of satellite imagery to detect small, scattered spots of infestation for suppression activities. They applied an unsupervised classification approach, with later assignment of mortality classes using a calibration dataset of interpreted aerial photos, to map mortality using IKONOS imagery (4 m spatial resolution), and found accuracies of 71% and 92% for low and medium levels of red-attack damage, respectively.

Our estimate of 31% mortality is a measure of trees with red foliage at the time of the 2005 image we analysed. This estimate is low compared with other published field observations of tree mortality following bark beetle attack. For example, Romme *et al.* (1986) reported tree mortality rates of 41–67% following a mountain pine beetle epidemic in the Greater Yellowstone Ecosystem. Other studies have found similarly high mortality, particularly in the large tree size classes (Amman and Baker 1972, Jorgensen and Mocettini 2005). Two likely reasons explain our lower estimates. First, total whitebark pine mortality in this area will increase with the continuing outbreak (as confirmed by field visits in 2006 and 2007). Secondly, our spatial extent was at the landscape, not plot, scale. At finer scales in some locations, the imagery classification resulted in much higher mortality rates (figure 6(d)). As larger areas contain more unattacked stands, we would expect the severity to decrease as area increases. Thus, a scene-wide 31% is likely a severe outbreak event. We note that because canopy cover – what the satellite observes – is dominated by larger trees that are preferentially attacked by mountain pine beetle, we might expect even higher mortality rates in terms of canopy cover compared to number of trees for these field studies.

6. Conclusions

This study used high spatial resolution, multi-spectral Quickbird imagery acquired in 2005 to identify mountain pine beetle-caused mortality in a high-elevation whitebark pine ecosystem in central Idaho, USA. We addressed multiple challenging aspects of mapping mountain pine beetle-caused mortality to achieve an accurate classification. Highly variable (i.e. discontinuous) forest canopy cover implied that the classification method needed to account for herbaceous vegetation. To accomplish this, we used RGI but also added the green reflectance (R_g). In addition, the mountainous terrain caused substantial variability in solar incidence angle, which resulted in variations in brightness within the region. Inclusion of the solar incidence angle in the image classification accounted for these variations. Finally, the steep, rugged terrain and minimal human influence on the landscape made spatial georegistration of the satellite imagery with ground-based observations difficult. By adding a buffer around

field measurements of dead and live trees, we accounted for uncertainties in image registration.

The widespread area of outbreaks at the regional and continental scales in remote, mountainous terrain poses challenges for mapping these important forest disturbances. Our results suggest that high-resolution satellite imagery can be used for monitoring insect infestations and for landscape ecological studies of tree mortality in these regions. Insect outbreaks have significant effects on ecosystem processes and services, and mapping the extent of these disturbances is crucial for fully assessing impacts.

Acknowledgements

The authors would like to thank Alistair Smith, Paul Gessler and Lee Vierling for helpful discussions and two anonymous reviewers whose comments improved the paper. This study was supported by the USDA Forest Service (03-CS-11222033-315, 06JV11221668274), the NSF-Idaho EPSCoR Program and the National Science Foundation (EPS-0447689), and the USGS through the Western Mountain Initiative (04CRAG0004/4004CS0001).

References

- AMMAN, G.D. and BAKER, B.H., 1972, Mountain pine beetle influence on lodgepole pine stand structure. *Journal of Forestry*, **70**, 204–209.
- AMMAN, G.D. and COLE, W. E., 1983, *Mountain Pine Beetle Dynamics in Lodgepole Pine Forests. Part II: population dynamics* (USDA Forest Service, GTR-INT-145).
- BETHLAHMY, N., 1974, More streamflow after a bark beetle epidemic. *Journal of Hydrology*, **23**, pp. 185–189.
- BRITISH COLUMBIA MINISTRY OF FORESTS AND RANGE, 2007, *2006 Summary of Forest Health Conditions in British Columbia*. Pest Management Report 15.
- CAYLOR, J., MEGOWN, J., FINCO, M., CALLEJAS, J., BOLLENBACHER, B. and MOISEN, G., 2002, *Large Scale Photography: An Initial Look at the Application and Results of Large Scale Photography in the New Millennium* (USDA Forest Service Remote Sensing Applications Center, RSAC-4001-RPT1).
- CHAN-MCLEOD, A.C.A., 2006, A review and synthesis of the effects of unsalvaged mountain-pine-beetle-attacked stands on wildlife and implications for forest management. *BC Journal of Ecosystems and Management*, **7**, pp. 119–132.
- COOPS, N.C., JOHNSON, M., WULDER, M.A. and WHITE, J.C., 2006, Assessment of QuickBird high spatial resolution imagery to detect red attack damage due to mountain pine beetle infestation. *Remote Sensing of Environment*, **103**, pp. 67–80.
- FRANKLIN, S.E., WULDER, M.A., SKAKUN, R.S. and CARROLL, A.L., 2003, Mountain pine beetle red-attack forest damage classification using stratified Landsat TM data in British Columbia, Canada. *Photogrammetric Engineering and Remote Sensing*, **69**, pp. 283–288.
- GIBSON, K.E., 2006, *Mountain Pine Beetle Conditions in Whitebark Pine Stands in the Greater Yellowstone Ecosystem, 2006* (USDA Forest Service, Northern Region, Missoula. Forest Health Protection Report R1Pub06-03).
- HICKE, J.A. and JENKINS, J.C., 2008, Mapping lodgepole pine stand structure susceptibility to mountain pine beetle attack across the western United States. *Forest Ecology and Management*, **225**, pp. 1536–1547.
- HICKE, J.A., LOGAN, J.A., POWELL, J. and OJIMA, D.S., 2006, Changing temperatures influence suitability for modeled mountain pine beetle (*Dendroctonus ponderosae*) outbreaks in the western United States. *Journal of Geophysical Research-Biogeosciences*, **111**, G02019, DOI: 02010.01029/02005JG000101.

- JENKINS, M.J., HEBERTSON, E., PAGE, W. and JORGENSEN, C.A., 2008, Bark beetles, fuels, fires and implications for forest management in the Intermountain West. *Forest Ecology and Management*, **254**, pp. 16–34.
- JORGENSEN, C.L. and MOCETTINI, P., 2005, *Monitoring Mountain Pine Beetle-Caused Mortality of Lodgepole Pine in the Sawtooth and Bear Valleys of South Central Idaho, 2004* (USDA Forest Service, FHP BFO-PR-05-01).
- KEANE, R.E. and ARNO, S.F., 1993, Rapid decline of whitebark pine in western Montana: Evidence from 20-year remeasurements. *Western Journal of Applied Forestry*, **8**, pp. 44–47.
- KNEPPECK, I.D. and AHERN, F.J., 1989, A comparison of images from a pushbroom scanner with normal color aerial photographs for detecting scattered recent conifer mortality. *Photogrammetric Engineering and Remote Sensing*, **55**, pp. 333–337.
- KURZ, W.A. and APPS, M.J., 1999, A 70-year retrospective analysis of carbon fluxes in the Canadian forest sector. *Ecological Applications*, **9**, pp. 526–547.
- KURZ, W.A., DYMOND, C.C., STINSON, G., RAMPLEY, G.J., NEILSON, E.T., CARROLL, A.L., EBATA, T. and SAFRANYIK, L., 2008, Mountain pine beetle and forest carbon feedback to climate change. *Nature*, **452**, pp. 987–990.
- LOGAN, J.A. and BENTZ, B.J., 1999, Model analysis of mountain pine beetle (Coleoptera: Scolytidae) seasonality. *Environmental Entomology*, **28**, pp. 924–934.
- LOGAN, J.A. and POWELL, J.A., 2001, Ghost forests, global warming and the mountain pine beetle (Coleoptera: Scolytidae). *American Entomologist*, **47**, pp. 160–173.
- LOGAN, J.A. and POWELL, J.A., in press, Ecological consequences of climate change altered forest insect disturbance regimes. In *Climate Change in Western North America: Evidence and Environmental Effects*, F.H. Wagner (Ed.), (Salt Lake City, Utah: University of Utah Press).
- LOGAN, J., REGNIERE, J. and POWELL, J.A., 2003, Assessing the impacts of global warming on forest pest dynamics. *Frontiers in Ecology and the Environment*, **1**, pp. 130–137.
- PERKINS, D.L. and SWETNAM, T.W., 1996, A dendroecological assessment of whitebark pine in the Sawtooth–Salmon River region, Idaho. *Canadian Journal of Forest Research-Revue Canadienne De Recherche Forestiere*, **26**, pp. 2123–2133.
- RADELOFF, V.C., MLADENOFF, D.J. and BOYCE, M.S., 1999, Detecting jack pine budworm defoliation using spectral mixture analysis: Separating effects from determinants. *Remote Sensing of Environment*, **69**, pp. 156–169.
- RICHARDS, J.A. and JIA, X., 2006, *Remote Sensing Digital Image Analysis* (Berlin: Springer-Verlag).
- ROMME, W.H., CLEMENT, J., HICKE, J., KULAKOWSKI, D., MACDONALD, L.H., SCHOENNAGEL, T.L. and VEBLEN, T.T., 2006, *Recent Forest Insect Outbreaks and Fire Risk in Colorado Forests: A Brief Synthesis of Relevant Research* (Colorado State University: Colorado Forest Restoration Institute).
- ROMME, W.H., KNIGHT, D.H. and YAVITT, J.B., 1986, Mountain pine beetle outbreaks in the Rocky Mountains – regulators of primary productivity. *American Naturalist*, **127**, pp. 484–494.
- SAFRANYIK, L. and CARROLL, A., 2006, The biology and epidemiology of the mountain pine beetle in lodgepole pine forests. In *The Mountain Pine Beetle: a Synthesis of Biology, Management, and Impacts on Lodgepole Pine*, L. Safranyik and W.R. Wilson (Eds), pp. 3–66 (Victoria, British Columbia: Natural Resources Canada, Canadian Forest Service, Pacific Forestry Centre).
- SKAKUN, R.S., WULDER, M.A. and FRANKLIN, S.E., 2003, Sensitivity of the thematic mapper enhanced wetness difference index to detect mountain pine beetle red-attack damage. *Remote Sensing of Environment*, **86**, pp. 433–443.
- USDA FOREST SERVICE, 2002, *Western Bark Beetle Report: A Plan to Protect and Restore Western Forests* (USDA Forest Service in cooperation with the Western Forestry Leadership Coalition).

- USDA FOREST SERVICE, 2005, *Forest Insect and Disease Conditions in the United States, 2004* (Washington, D.C.: USDA Forest Service).
- VAN SICKLE, G.A., 1995, Canadian aerial surveys for pest damage assessment. In *Aerial Pest Detection and Monitoring Workshop*, pp. 24–27 (Las Vegas, NV: USDA Forest Service).
- VERMOTE, E.F., TANRE, D., DEUZE, J.L., HERMAN, M. and MORCRETTE, J.J., 1997, Second Simulation of the Satellite Signal in the Solar Spectrum, 6S: An overview. *IEEE Transactions on Geoscience and Remote Sensing*, **35**, pp. 675–686.
- WHITE, J.C., WULDER, M.A., BROOKS, D., REICH, R. and WHEATE, R.D., 2005, Detection of red attack stage mountain pine beetle infestation with high spatial resolution satellite imagery. *Remote Sensing of Environment*, **96**, pp. 340–351.
- WULDER, M.A., DYMOND, C.C., WHITE, J.C., LECKIE, D.G. and CARROLL, A.L., 2006, Surveying mountain pine beetle damage of forests: A review of remote sensing opportunities. *Forest Ecology and Management*, **221**, pp. 27–41.
- WULDER, M.A., WHITE, J.C., COOPS, N.C. and BUTSON, C.R., 2008, Multi-temporal analysis of high spatial resolution imagery for disturbance monitoring. *Remote Sensing of Environment*, **112**, pp. 2729–2740.